Title

Stemness genes and miR-1247-3p expression associate with clinicopathological parameters and prognosis in lung adenocarcinoma.

Permalink

Journal

Authors

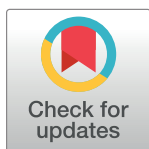Limbu, Shiwani

McCloskey, Kara

Publication Date

2023

DOI

Peer reviewed

PLOS ONE

Stemness genes and miR-1247-3p expression associate with clinicopathological parameters and prognosis in lung adenocarcinoma

Shiwani Limbu[1], Kara E. McCloskey[1,2]*

1 Quantitative and System Biology Program, University of California, Merced, Merced, CA, United States of America, 2 Materials Science and Engineering Department, University of California, Merced, Merced, CA, United States of America

* kmccloskey@ucmerced.edu

Abstract

Lung cancer makes up one-fourth of all cancer-related mortality with the highest mortality rate among all cancers. Despite recent scientific advancements in cancer therapeutics, the 5-year survival rate of lung adenocarcinoma (LUAD) cancer patients remains below 15 percent. It has been suggested that the high mortality rate of LUAD is linked to the acquisition of progenitor-like cells with stem-like characteristics that assist the whole tumor in regulating immune cell infiltration. To examine this hypothesis further, this study mined several databases to explore the presence of stemness-related genes and miRNAs in LUAD cancers. We examine their association with immune and accessory cell infiltration rates and patient survival. We found 3 stem cell-related genes, ORC1L, KIF20A, and DLGAP5, present in LUAD that also correlate with changes in immune infiltration rates and reduced patient survival rates. Additionally, the modulation in myeloid-derived suppressor cell (MDSC) infiltration and miRNA hsa-mir-1247-3p mediated targeting of tumor suppressor SLC24A4 and oncogenes RAB3B and HJURP appears to primarily regulate LUAD patient survival. Given these findings, hsa-mir-1247-3p and/or its associated gene targets may offer a promising avenue to enhance patient survivability.

Introduction

Lung cancer corresponds to 25% of all cancer deaths [1], the greatest mortality rate among all cancers [2]. The two most common types of lung cancer are lung adenocarcinoma (LUAD) and lung squamous cell carcinoma (LUSC) [3], with LUAD recently replacing squamous cell cancer as the most prevalent non-small cell cancer in the United States. Despite recent scientific advancements in the development of anti-cancer therapeutics, the 5-year survival rate of LUAD cancer patients remains less than 12% to 15% [4].

One hypothesis for the high mortality rate of LUAD is its ability to evade the body's immune system [5]. Cancer progression is marked by the de-differentiation of tissue-specific

cells and acquisition of progenitor-like cells with stem-like characteristics. These cancer stem cells (CSC) [6] are then able to assist the whole tumor [7] with proliferation, progression and propagation [8]. Moreover, stem cells and CSCs in cancers correlate with the rate and type of immune responses [9], tumor metastasis [10], multi-drug resistance [11], and low cancer patient survival [12, 13]. The relationship between CSCs, stem cell-related genes, and cancer therapeutics has been widely investigated in a number of cancers with respect to potential biomarkers [14, 15], the tumor microenvironment (TME) [15, 16], and immune cell infiltration [17, 18]. CSCs have also been shown to be resistant to traditional therapies, correlating with enhanced epithelial to mesenchymal (EMT) properties, reduced DNA repair mechanisms, enhanced expression of ATP-binding cassette (ABC) membrane transporters, activation of several survival signaling pathways, and increased immune evasion [19].

Because immune cell infiltration affects cancer progression [20–22], immune cells have been proposed as possible delivery vehicles for gene therapy [23]. HSCs can infiltrate tumors to fight disease progression, but exhibit only limited infiltration in lung tumors [24]. Conversely, immune cells that enable cancer progression include MDSCs that can suppress T cell activation, induce other immune-suppressive cell populations, regulate inflammation, and promote the switching of the immune system to tolerate tumor growth [25, 26], and Th2 T cell CD4+ (Th2) cells promotes angiogenesis and inhibit cytotoxic T-cell immune responses [27]. Th2 cells regulate humoral immune response and produce interleukin 4 and 10 [28], which in turn reduces the normal Th1 cytotoxic activity [28] that can kill cancer cells [29]. Moreover, a negative relationship between cancer patient survival probability and Th2 infiltration rates has been demonstrated in LUAD patients [22, 30].

In addition to immune cell infiltration, the production of inflammatory molecules and other changes in gene expression and microRNAs (miRNAs) can act as a key cell signaling molecules in cancer initiation and metastasis [31]. miRNAs can change gene expression by inhibiting or promoting mRNA translation, stability, or degradation [32]. Therefore, changes in expression levels of miRNA can promote or inhibit tumorigenesis by altering the expression of tumor suppressors and oncogenes [33, 34]. Most recently, CSC-associated drug resistance and metastasis are being specifically targeted (reviewed in [35]) as potential treatment options. Current strategies for targeting CSCs in cancer include small molecule inhibitors, immunotherapy, microRNA mediated inhibitors, epigenetic methods as well as targeting CSC niche-microenvironmental factors and differentiation.

To capture and integrate the long list of potential factors associated with tumor progression and patient survivability, bioinformatics methods are gaining traction in the study of large gene sets, including stem cell-related gene in cancer cells [10], aimed at identifying new therapies for treating resistant cancers. Malta et. al, used an innovative one-class logistic regression (OCLR) machine-learning algorithm [36] to extract transcriptomic and epigenetic feature sets derived from pluripotent stem cells and differentiated cells, and found biological mechanisms associated with a dedifferentiated oncogenic state, called the *stemness index*. Two independent stemness indices were found, a methylated DNA stemness index (mDNAsi) highlighted the epigenetic features of the cells and a messenger RNA stemness index (mRNAsi) indicating gene expression [10]. The associations between the two stemness indices highlighted novel oncogenic pathways, somatic alterations, miRNAs and transcriptional regulatory networks, and revealed a strong negative correlation between cancer stemness and infiltrating immune cells in the tumors [10]. These advancements in bioinformatics methods, stemness index has been applied to identify key biomarkers and potential therapeutic strategies associated with cancer [30, 37–42].

Using the recently reported stem cell-related biomarkers in cells from LUAD patients [30, 43, 44]. We explored the relationship between stemness related gene and miRNA expression,

and immune infiltration rates in the TMEs of LUAD patients and patient survival probability. We found that the increased expression of stemness related genes in LUAD correlated with reduced immune cell infiltration and reduced patient survivability. We also identified modulation of MDSC infiltration and hsa-miR-1247-3p expression as a key regulators in LUAD patient survival rates, potentially biomarkers for diagnoses and treatment in LUAD patients.

Methods

Data collection

We used 109 stem cell-related genes indicating tumor stemness from cancer transcriptomes using single-sample gene set enrichment analysis (ssGSEA) from cancer transcriptomes [9]. Gene and miRNA expression data of 537 LUAD tumor and 59 normal samples were collected from The Cancer Genome Atlas (TCGA) database [45], and two more microarray gene expression datasets were obtained from GEO database [46] (GSE ID: GSE40419 and GSE31210) and used as a validation cohort for gene differential expression test. Here GSE40419 contains 87 tumor samples and 77 normal samples, whereas GSE31210 contains 226 tumor samples and 20 normal samples. Tumor patient cancer stage (I, II, III, and IV), patient age, and LUAD specific patients survival duration (in months) were collected from cBioPortal [47].

Differential expression test

A differential expression test of TCGA gene and miRNA expression data was performed using DeSeq2 [48] to detect differentially expressed genes and miRNA in LUAD cancer. Limma [49] was used to perform differential expression test on microarray gene expression data obtained from GEO database. Differentially expressed genes and miRNA were identified using Benjamini and Hochberg (BH) adjusted *p-value* cutoff < = 0.05 and *log2 foldchange* (LFC) >2 or LFC < –2. Here, the *foldchange* in gene and miRNA expression corresponds to the ratio between expression in cancer compared with normal samples.

Univariate Cox-proportional hazard model-based survival analysis

Cox-proportional hazard model [50] was implemented to calculate a hazard ratio, which corresponds to the relationship between the change in expression of a gene in cancer samples and patient survival probability. A hazard rate is defined as the likelihood of experiencing a hazardous event, such as increased disease progression or death, during a defined duration time [50]. We divided patient clinical assessment and gene expression data into high and low gene expression groups and calculated a hazard rate for both groups. A hazard ratio was then calculated from the hazard rate obtained from high expression group and low expression groups. A hazard ratio greater than 1.0, with adjusted *p-value* less than 0.05, indicated a reduced probability of patient survival in the group containing higher expression of stemness genes. This step, known as survival analysis, was performed using Timer2.0 [51]. The *p-values* obtained from survival analysis were adjusted for multiple tests using Benjamini and Hochberg method. The genes with adjusted *p-value* less than 0.05 were selected as markers associated with the loss of patient survival in LUAD for downstream analysis.

Immune infiltration test

Immune infiltration profile and its association with gene expression in LUAD patient samples were obtained from Timer2.0 (http://timer.cistrome.org/) [51], a comprehensive resource that includes data on immune and accessory cell infiltration calculated using TCGA gene expression data through various computational methods such as Timer [52], TIDE [53], MCP-

counter [54], quanTIseq [55], xCell [56], CIBERSORT [57], Epic [58], and immunedeconv [59]. Computationally predicted LUAD tumor infiltration rate of a total of 32 immune and accessory cell types were examined in this study including endothelial cell, cancer associated fibroblasts, hematopoietic stem cells (HSCs), memory B cells, naïve B cell, plasma B cell, naive T cell CD4+, central memory T cell CD4+, effector memory T cell CD4+, Th1 T cell CD4+ (Th1), Th2, naive T cell CD8+, central memory T cell CD8+, effector memory T cell CD8+, Tregs, neutrophils, monocytes, macrophage M0, macrophage M1, macrophage M2, myeloid dendritic cells, plasmacytoid dendritic cells, natural killer (NK) cells, mast cells, common lymphoid progenitors, common myeloid progenitors, granulocyte-monocyte progenitor, eosinophils, T cell follicular helper, T cell gamma delta, natural killer T cell, myeloid derived suppressor cells (MDSCs). Here, immune cells with correlation greater than 0.6 or less than -0.6, and p-value < = 0.05, were used as a selection cutoff to identify highly correlated gene expression and immune cell infiltration rate pairs. Cox-proportional hazard model test and Kaplan-Meier curve calculation results were also obtained from Timer2.0 to test the relationship between high and low immune cell infiltration rates and LUAD cancer patient survival.

Identification of miRNAs binding to the 3' UTR region of marker genes

All miRNAs binding to 3' UTR region of genes were identified using mirWalk [60]. Along with miRNA-gene 3' UTR binding prediction, mirWalk looks for validated miRNA-gene binding from miRTarBase [61]. In this study, the 3p and 5p variants of miRNA that bind to the 3' UTR region of the differentially expressed stemness-related genes were identified and selected using mirWalk and annotated as known gene targeting miRNAs in miRTarBase database. The stemness genes targeting miRNAs that exhibited a LFC greater than 2 or less than -2, with BH adjusted p-value ≤ 0.05 in both DeSeq2 and Limma differential expression tests were selected for further downstream analysis.

Multivariate Cox-proportional hazard model-based survival analysis

Multivariate Cox-proportional hazard model-based survival analysis was performed to calculate contribution of key factors to change in patient survival rate. The data set consisted of various predictors, including patient age, cancer stages, patient survival duration after being diagnosed with LUAD, genes expression level, miRNAs expression level, and computationally predicted immune cell infiltration rates. Here, MDSC infiltration rates were collected from Tide [62]. Computationally predicted infiltration data of HSC and T-cell CD4+ Th2 (Th2) was obtained from Timer2.0 database. Multivariate Cox-proportional hazard model analysis was conducted using Survival Analysis package in R. This comprehensive approach allowed us to account for the complex interplay between the variables and their effects on cancer patient survival rate.

Results

Stemness genes associated with cancer patient survival

Out of total 109 stemness related genes obtained from Miranda et al., 2019 [9], four (ORC1L, KIF20A, DLGAP5, and RAB3B) genes were found to be differentially expressed in LUAD cancer using datasets TCGA, GSE40419, and GSE31210, hazard ratio > 1. Benjamini and Hochberg (BH) adjusted p-value ≤ 0.05 (Table 1). Due to their likely role in promoting cancer progression, ORC1L, KIF20A, DLGAP5, and RAB3B were selected as marker genes for downstream analysis.

Table 1. Differentially expressed stemness genes and regression coefficients obtained from survival analysis. Here, positive log foldchange change (LFC) corresponds to upregulated genes and negative log foldchange corresponds to downregulated genes. LUAD cancer patient data is divided into high expression and low expression groups, with low gene expression used as reference values when performing Cox-proportional hazard model analysis [51] in Timer 2.0. The hazard ratio for each gene represents the impact of the corresponding gene expression change observed in high expression sample as compared to the low expression samples within the tumor samples. Genes with log foldchange greater than 2 or less than -2 across TCGA using DeSeq2 and GSE40419 datasets and GSE31210 dataset using Limma, and with hazard ratio greater than 1 with Benjamini and Hochberg (BH) adjusted p-value less than 0.05 is selected as key genes that are associated with loss of cancer patient survival. If gene differential expression test BH adjusted p-value is not smaller than 0.05, then it is represented with ns.

|	Differential expression test log foldchange				Survival Analysis		
Dataset	TCGA	TCGA	GSE40419	GSE31210	Hazard ratio	p-value	BH adjusted p-value
Method	DeSeq2	Limma	Limma	Limma			
DLGAP5	3.671	5.411	4.184	3.003	1.314	0.0	0.0
KIF20A	3.143	4.791	3.912	2.211	1.314	0.0	0.0
CENPI	2.740	3.907	2.719	ns	1.225	0.013	0.02785
ORC1L	2.741	4.081	2.564	2.530	1.263	0.002	0.006
IGF2BP1	6.589	4.805	3.485	ns	1.272	0.0	0.0
HMGA2	5.761	4.583	4.192	ns	1.14	0.001	0.00375
RAB3B	4.242	4.785	3.152	2.065	1.181	0.026	0.04875
DNMT3B	2.046	2.836	1.536	0.601	1.109	0.131	0.17863
SOHLH2	4.433	3.367	2.588	ns	1.021	0.727	0.77892
FGF2	-2.009	-3.058	-2.269	-0.828	1.217	0.11	0.165
MYCN	3.378	2.916	0.834	ns	0.94	0.275	0.32307
INHBE	4.239	3.322	0.809	ns	0.97	0.813	0.813
NMNAT2	2.735	2.252	0.771	ns	1.052	0.28	0.32307
LIN28B	7.632	5.190	3.884	ns	1.238	0.047	0.07833
ALX1	3.189	2.699	1.372	ns	1.286	0.007	0.0175

https://doi.org/10.1371/journal.pone.0294171.t001

Stemness genes and immune cell infiltration

Three stemness-related gene (ORC1L, KIF20A, DLGAP5) positively correlated (> 0.6) with the infiltration rate of Th2 and MDSC. ORC1L negatively correlated with hematopoietic stem cell (HSC) infiltration rate (< -0.6) (Fig 1). Cox-proportional hazard Model-based survival analysis coefficients obtained from Timer2.0 indicated a higher infiltration rate of both Th2 and MDSCs in three genes (ORC1L, KIF20A, and DLCAP5) corresponding to a lower patient survival rate. RAB3B did not exhibit a correlation with any immune and accessory cell infiltration rate within the correlation cutoff range. Moreover, higher infiltration rate of HSCs corresponded to higher patient survival rate (Table 2).

miRNAs regulating stemness genes

From cross-referencing the mirWalk and miRTarBase database [61], total five miRNAs (hsa-mir-197-3p, hsa-mir-1247-3p, hsa-mir-122-5p, hsa-mir-215-5p, hsa-mir-192-5p) were differentially expressed in TCGA dataset DeSeq2 results, all targeting 3' UTR region of RAB3B (Table 3). No miRNAs targeting ORC1L, KIF20A, and DLGAP5 3' UTR regions were differentially expressed in TCGA dataset in DeSeq2 analysis results. Differential expressions of these 5 miRNAs in the TCGA dataset were also conducted using Limma to remove potential false positives. As RAB3B is upregulated in LUAD, downregulated miRNAs with Limma LFC less than -2, and BH adjusted p-value ≤0.05, were selected for downstream analysis. Out of these 5 miRNAs, only one, hsa-mir-1247-3p, exhibited the Limma LFC and BH adjusted p-value within the cutoff criteria (Table 3).
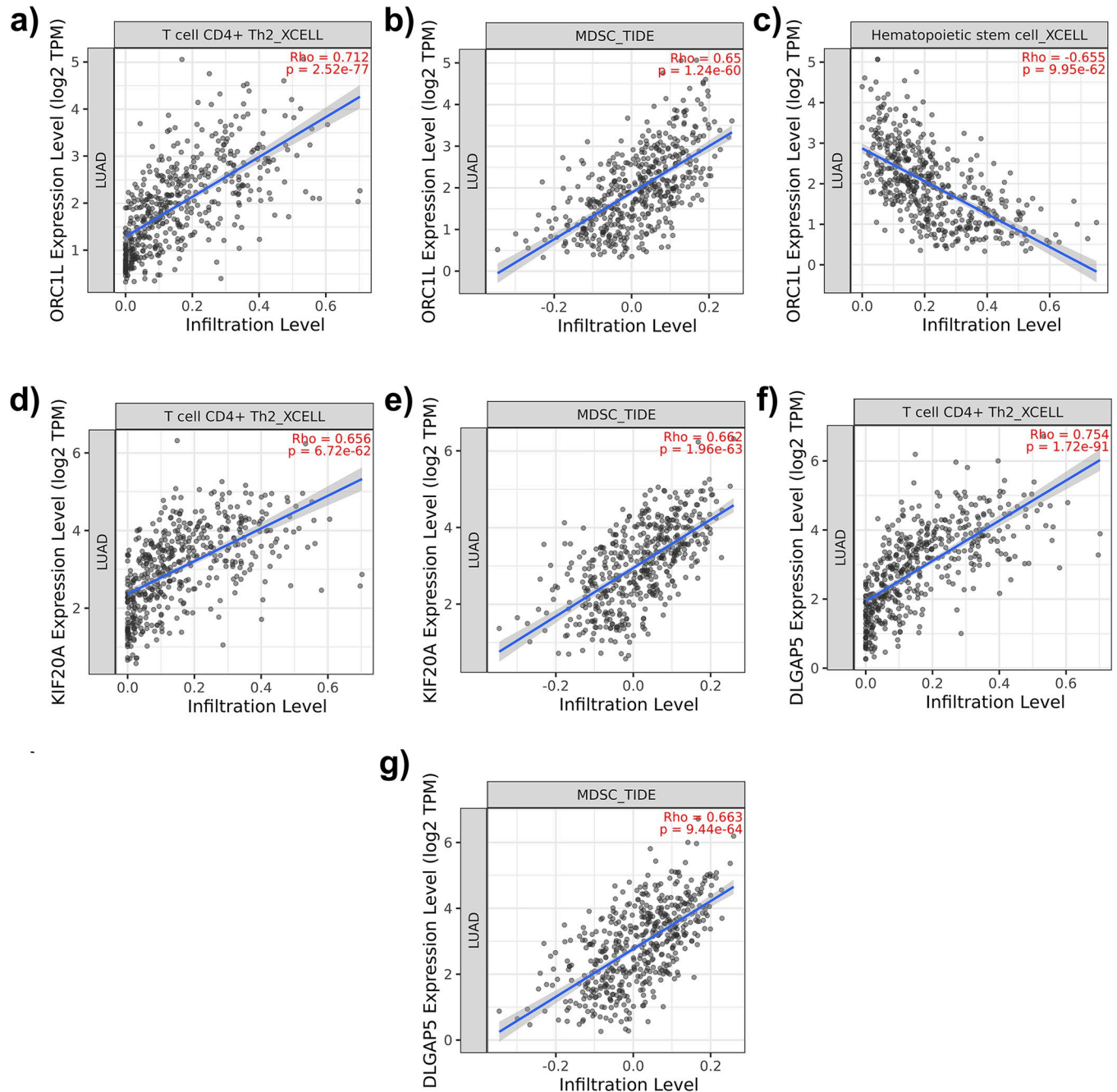
Fig 1. Immune cell infiltration profiles. a) correlation between T cell CD4+ Th2 (Th2) cells infiltration rate and ORC1L gene expression, b) correlation between MDSC infiltration rate and ORC1L gene expression, c) correlation between HSC infiltration rate and ORC1L gene expression, d) correlation between Th2 cells infiltration rate and KIF20A gene expression, e) correlation between MDSCs infiltration rate and KIF20A gene expression, f) correlation between Th2 cells infiltration rate and DLGAP5 gene expression, g) correlation between MDSCs infiltration rate and DLGAP5 gene expression.

Key markers of LUAD

Multivariate Cox-proportional hazard model analysis was first conducted using hsa-mir-1247-3p, KIF20A, RAB3B, ORC1L, and DLGAP5 expression, MDSC, Th2, and HSC infiltration, LUAD cancer patient age and cancer stage as covariates to identify key markers promoting loss of patient survival rate. Results (Table 4) indicate that although hsa-mir-1247-3p was

Table 2. Hazard ratio and p-value of Cox-proportional hazard model test for Th2, MDSC, and HSC cell immune infiltration rate with patient survival report.
Here, LUAD cancer patient data is divided into high and low infiltration groups with low immune cell infiltration is used as reference value when performing Cox-proportional hazard model analysis in Timer2.0 [51].

Factor name	Reference value	Factor value	Hazard ratio	pvalue	BH adjusted p-value
Th2	Low infiltration	High infiltration	3.804	0.006	0.009
MDSC	Low infiltration	High infiltration	62.036	0	0
HSC	Low infiltration	High infiltration	0.167	0.046	0.046

downregulated in LUAD, increases in hsa-mir-1247 expression within the cancer patient samples lead to loss of survival rate (Table 4). Furthermore, the increase in infiltration of MDSC is also shown to be associated with LUAD loss of survival rate (Table 4). No significant correlation (Pearson correlation score = -0.05) between MDSC, and hsa-mir-1247-3p was observed. Furthermore, as expected, cancer stage II, III, and IV and increased age are significantly associated with a decrease in cancer patient survival rate (Table 4). These results suggest that modulation of hsa-mir-1247-3p expression and MDSC infiltration significantly contributed to the loss of patient survival in LUAD, but likely use distinctly different mechanisms.

Role of hsa-mir-1247-3p target genes in LUAD

A total of 53 genes were identified as common targets of has-mir-1247-3p in both the mirWalk and mirTarBase databases (S1 Table). Differential expression analysis of the TCGA, GSE40419, and GSE31210 datasets of these 53 genes, utilizing both DeSeq2 and Limma methods, showed that HJURP and RAB3B consistently exhibited a LFC greater than 2.0 across all datasets (S2 Table). Additionally, SLC24A4 showed an LFC of less than -2.0 across all three datasets when analyzed with the Limma, and an LFC of -1.98158 when assessed using the DeSeq2 (S2 Table). These results indicate that in addition to RAB3B, two other hsa-mir-1247-3p target genes HJURP and SLC24A4, are also significantly differentially expressed across all examined datasets and methodological approaches. Like expression trends of ORC1L, HJURP exhibited significant positive correlation with Th2 and MDSC, and a significant negative correlation with HSC (Fig 2). However, SLC24A4 did not exhibit a correlation greater than 0.6 or less than -0.6 with any immune and accessory cell infiltration rates. Additionally, hsa-mir-1247-3p, binding to the 3' UTR region of the STAT5A gene, has also been suggested to play a role in reducing the progression of LUAD [63]. Here, univariate Cox-proportional hazard model analysis results obtained from Timer2.0 database indicates that change expression of HJURP and SALC24A4 is significantly associated with loss of LUAD cancer patient survival rate, whereas STAT5A exhibited a weaker association trend with patient survival rate (Table 5). A multivariate Cox-proportional hazard model analysis incorporating factors including hsa-mir-1247-3p, RAB3B, HJURP, SLC24A4, and STAT5A expression, cancer stage,

Table 3. Log2 foldchange (LFC) and Benjamini/Hochberg (BH) adjusted p-value obtained from DeSeq2 and Limma for 5 miRNAs. Here, miRNAs with both DeSeq2 and Limma log foldchange greater than 2 or less than -2, and BH adjusted p-value ≤0.05 were selected for downstream analysis.

miRNAs		DeSeq2		Limma	
	RAB3B binding miRNA variant	LFC	BH adjusted p-value	LFC	BH adjusted p-value
hsa-mir-1247	3p	-2.324	3.51E-19	-3.151	1.63E-11
hsa-mir-192	5p	3.162	1.62E-21	2.715	4.19E-08
hsa-mir-122	3p	1.806	9.95E-08	2.007	0.245932
hsa-mir-215	5p	2.135	2.51E-09	0.655	0.245932
hsa-mir-197	3p	-2.965	1.58E-79	0.130	0.628424

Table 4. Multivariate Cox-proportional hazard model analysis results highlighting key markers associated with increase in patient mortality rate. Here, LUAD patient tumor samples are divided into low and high infiltration groups for immune cell infiltration, low and high expression groups for gene and miRNA expression, and low and high age groups for LUAD cancer patient age. Reference values used for multivariate Cox-proportional hazard model analysis for each factor are shown in the table.

Factor name	Reference value	Factor value	HR	p-value
Cancer stage	STAGE I	STAGE III	3.17373	6.30E-08
Cancer stage	STAGE I	STAGE IV	3.627736	2.46E-05
Cancer stage	STAGE I	STAGE II	1.941041	0.001473
hsa-mir-1247-3p	High expression	Low expression	0.667653	0.02279
MDSC	High infiltration	Low infiltration	0.655898	0.028825
Age	High	Low	0.740296	0.071889
Th2	High infiltration	Low infiltration	0.829268	0.361647
KIF20A	High expression	Low expression	0.807105	0.428903
RAB3B	High expression	Low expression	0.892945	0.536809
HSC	High infiltration	Low infiltration	1.048088	0.827427
ORC1L	High expression	Low expression	0.964545	0.881234
DLGAP5	High expression	Low expression	0.981126	0.944834

https://doi.org/10.1371/journal.pone.0294171.t004

patient age, and MDSC, Th2, and HSC infiltration rates, was conducted to assess the specific influence of HJURP, SLC24A4, and STAT5A on patient survival. Genes HJURP, STAT5A, and SLC24A4, like RAB3B, also failed to demonstrate a significant trend of association with the loss of patient survival rate (Table 6).

Discussion and conclusions

Using predefined stemness-related genes and cross-referencing these against the LUAD patients, we found 15 differentially expressed stemness-related genes in LUAD. Of these, four genes (ORC1L, KIF20A, DLGAP5, and RAB3B) underlined negatively correlated with the probability of patient survival (Table 1 and Fig 1). We then examined the immune cell infiltration in LUAD cancer patients and found a decreased infiltration rate of HSCs and increased infiltration of MDSC and Th2 cells correlating with decreased survival probability correlating with three genes (ORC1L, KIF20A, and DLGAP5—Fig 1). Lastly, the examination of stemness-related genes and immune cell infiltration rates in LAUD patients linked the increase in expression of ORC1L with the negatively correlated infiltration rate of HSC (Fig 2C) but did not suggest a strong correlation between Th2 infiltration or other differentially expressed stemness-related genes.
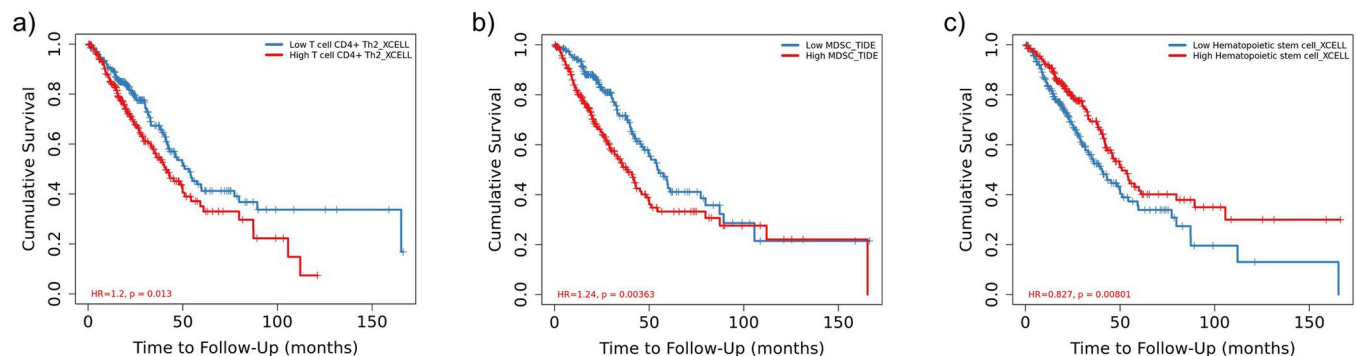
Fig 2. Immune cell infiltration profiles. a) correlation between T-cell CD4+ Th2 (Th2) cells infiltration rate and HJURP gene expression, b) correlation between MDSC infiltration rate and HJURP gene expression, c) correlation between HSC infiltration rate and HJURP gene expression.

https://doi.org/10.1371/journal.pone.0294171.g002

Table 5. Hazard ratio and p-value of Cox-proportional hazard model test for HJURP, SLC24A4, and STAT5A expression with patient survival report. Here, LUAD cancer patient data is divided into high and low and high expression groups, where low expression is used as reference value when performing Cox-proportional hazard model analysis in Timer2.0 [51].

Factor name	Reference value	Factor value	HR	p-value
HJURP	Low expression	High expression	1.29	0
SLC24A4	Low expression	High expression	0.399	0.013
STAT5A	Low expression	High expression	0.868	0.14

https://doi.org/10.1371/journal.pone.0294171.t005

ORC1L is a highly conserved six subunit protein, which plays an important role in regulating initiation of DNA replication process during cell division [64] and organ development [65]. Recently, aberrations in ORC1L have been implicated in breast cancer [66], cervical cancer [67], as well as LUAD cancer progression [68]. Investigating the role of ORC1L more closely, we found that aberrations in ORC1L gene expression have been previously linked with LUAD tumor growth [68, 69] through changes in immune cell infiltration [68]. Han et al., [68] postulated that ORC1L promotes LUAD tumor progression and aberration of immune infiltration by deregulating WNT signaling pathway. Alterations of WNT signaling have been implicated in modulation of immune infiltration in cancer, thereby promoting tumor progression [70]. Therefore, the relationship between the upregulation of ORC1L and changes in immune infiltration and loss LUAD patient survival is likely driven by changes in the WNT signaling pathway.

As expected, our results also agreed with previous studies [22, 25–27, 30] showing that an increase in infiltration of MDSC and Th2 decreased the survival probability of cancer patients in LUAD (Fig 2). Uniquely, we found an increase in expression of ORC1L, KIF20A, and DLGAP5 stemness-related genes also positively correlated with MDSC and Th2 infiltration rates in LUAD cancer (Fig 1). Myeloid-derived suppressor cells (MDSCs) comprise a varied collection of undeveloped myeloid cells and play a crucial role in negatively modulating the immune response [71]. This regulation, combined with immune infiltration rates of T-helper Th2 cells, contributes to the advancement of tumors [71], the formation of pre-metastatic niches [72], and a decrease in the effectiveness of immunotherapy [71]. The underlying processes that achieve these functions are intricate and multifaceted, encompassing both immunosuppressive activities (such as the restraint of cytotoxic T-cells [73]) and non-immunological roles like facilitating stemness genes [74] and encouraging angiogenesis by

Table 6. Multivariate Cox-proportional hazard model analysis results of differentially expressed genes targeted by hsa-mir-1247-3p. Here, LUAD patient tumor samples are divided into low and high infiltration groups for immune cell infiltration, low and high expression groups for gene and miRNA expression, and low and high age groups for LUAD cancer patient age. Reference values used for multivariate Cox-proportional hazard model analysis for each factor are shown in the table.

Factor name	Reference value	Factor value	HR	p-value
Cancer stage	STAGE I	STAGE III	3.060216	1.49E-07
Cancer stage	STAGE I	STAGE IV	3.666859	2.08E-05
Cancer stage	STAGE I	STAGE II	1.938426	0.001264
hsa-mir-1247-3p	High expression	Low expression	0.675477	0.02661
MDSC	High infiltration	Low infiltration	0.681396	0.084532
Age	High	Low	0.763052	0.102087
HJURP	High expression	Low expression	0.709094	0.121995
Th2	High infiltration	Low infiltration	0.858448	0.456893
SLC24A4	High expression	Low expression	1.117642	0.579472
STAT5A	High expression	Low expression	0.926444	0.682518
RAB3B	High expression	Low expression	0.934566	0.712562
HSC	High infiltration	Low infiltration	1.039916	0.852716

https://doi.org/10.1371/journal.pone.0294171.t006

secreting various growth factors such as vascular endothelial growth factor (VEGF), basic fibroblast growth factor (bFGF), prokineticin-2 (Bv8), and platelet-derived growth factor (PDGF) [75]. The MDSC activation and expansion by stemness-related genes [26] has also been shown to negatively regulate the host's immune response by promoting release of cytokines and chemokines to protect cancer cells in many cancers [76]. Similarly, upregulation of KIF20A stemness-related gene is known to positively correlate with Th2, Treg cells and macrophage infiltration rates, and negatively correlate with Th17, mast cells and natural killer cells infiltration in renal cell carcinoma [77]. This meta-analysis confirmed the similar role for KIF20A in LUAD.

Looking more closely at the two mitosis related gene, DLGAP5, it has also been shown to be important in cancer prognosis [78, 79], but the mechanism associated with its impact on cancer progression remains unclear. This meta-analysis found the expression of DLGAP5 is positively correlated with Th2 and MDSC infiltration rate, as well as loss of patient survival probability, highlighting its role in promoting cancer progression. DLGAP5 is a microtubule associated protein, which maintains progression of normal cell division by regulating chromosomal rearrangement and gene stability [80]. Looking at current literature, the overexpression of DLGAP5 has been shown to increase cancer cell migration and invasion in gastric cancer [81].

Searching the miRNA database for potential miRNAs correlating positively with stemness-related genes in LUAD cancer, we found one miRNA (has-mir-1247-3p) targeting RAB3B, HJURP, SLC24A4, and STAT5A, all differentially expressed in LUAD. Previous reports on hsa-mir-1247-3p found it to be a key biomarker in pancreatic cancer [82], breast cancer [83], liver cancer [84], bone cancer [85], and neuroblastoma [86]. Moreover, deregulation of hsa-mir-1247-3p has been shown to lead to increased cancer progression [63] suggesting that it may play a role in mitigating cancer progression in LUAD cancers [63] (correlation coefficient -0.314, p-value 0.001 with STATA5A gene expression).

Despite the downregulation of hsa-mir-1247-3p in LUAD, the multivariate Cox-proportional hazard model analysis suggested that an increase in expression of hsa-mir-1247-3p within LUAD patients had a significant association with loss of patient survivability (Tables 4 and 5). Upon further investigation further, it seems that miRNAs are known to regulate oncogenes as well as tumor suppressors, and the balance between the two mediates direction of impact of tumor progression [87]. Results obtained from this study, and Lin et al., [63], indicate that hsa-mir-1247-3p targets LUAD differentially expressed oncogenes (RAB3B and HJURP), as well as differentially expressed tumor suppressors (SLC24A4 and STAT5A – Table 5). While the increase in expression of oncogenes RAB3B and HJURP and loss of expression of tumor suppressor SLC24A4 is associated with diminished cancer patient survivability, the downregulation of tumor suppressor STAT5A has been shown to promote tumor growth [63]. Moreover, hsa-mir-1247-3p modulation mediates the association between the change in expression of these genes and patient survival rate, acting as a key marker and central node in the regulatory network associated with tumor progression.

While traditionally considered as gene-regulatory elements, miRNAs—like hsa-mir-1247-3p - may also influence more complex signaling pathways within the tumor microenvironment. These analyses did not indicate a significant correlation between MDSC infiltration scores and hsa-mir-1247-3p expression, suggesting distinct regulatory mechanisms leading to their shared involvement in regulating patient survival rate.

Supporting information

S1 Table. List of genes targeted at 3' UTR region by hsa-mir-1247-3p obtained from mirWalk database [1]. Here, each gene-miRNA pair is a validated interaction with mirTarBase

[2] ID.
(DOCX)

S2 Table. Differential expression results of genes targeted by hsa-mir-1247-3p at 3' UTR regions. Here, log2 foldchange (LFC) and Benjamini and Hochberg (BH) adjusted p-values were obtained from DeSeq2 [1] and Limma [2] applied on TCGA [3] and GEO [4] datasets. (DOCX)

Author Contributions

Conceptualization: Shiwani Limbu.

Formal analysis: Shiwani Limbu.

Investigation: Shiwani Limbu.

Methodology: Shiwani Limbu.

Supervision: Kara E. McCloskey.

Validation: Kara E. McCloskey.

Writing – original draft: Shiwani Limbu.

Writing – review & editing: Kara E. McCloskey.

References

1. Siegel RL, Miller KD, Fuchs HE, Jemal A. Cancer Statistics, 2021. CA Cancer J Clin. 2021; 71: 7–33. https://doi.org/10.3322/caac.21654 PMID: 33433946

2. Siegel RL, Miller KD, Fuchs HE, Jemal A. Cancer statistics, 2022. CA Cancer J Clin. 2022; 72: 7–33. https://doi.org/10.3322/caac.21708 PMID: 35020204

3. Chen JW, Dhahbi J. Lung adenocarcinoma and lung squamous cell carcinoma cancer classification, biomarker identification, and gene expression analysis using overlapping feature selection methods. Sci Rep. 2021; 11: 13323. https://doi.org/10.1038/s41598-021-92725-8 PMID: 34172784

4. Myers DJ, Wallen JM. StatPearls. StatPearls Publishing. Treasure Island (FL); 2022. https://doi.org/10.1007/978-3-642-19677-5_22

5. Spella M, Stathopoulos GT. Immune resistance in lung adenocarcinoma. Cancers (Basel). 2021; 13: 1–17. https://doi.org/10.3390/cancers13030384 PMID: 33494181

6. Prager BC, Xie Q, Bao S, Rich JN. Cancer Stem Cells: The Architects of the Tumor Ecosystem. Cell Stem Cell. 2019; 24: 41–53. https://doi.org/10.1016/j.stem.2018.12.009 PMID: 30609398

7. Reya T, Morrison SJ, Clarke MF, Weissman IL. Stem cells, cancer, and cancer stem cells. Nature. 2001; 414: 105–111. https://doi.org/10.1038/35102167 PMID: 11689955

8. Prasad S, Ramachandran S, Gupta N, Kaushik I, Srivastava SK. Cancer cells stemness: A doorstep to targeted therapy. Biochim Biophys Acta—Mol Basis Dis. 2020; 1866: 165424. https://doi.org/10.1016/j.bbadis.2019.02.019 PMID: 30818002

9. Miranda A, Hamilton PT, Zhang AW, Pattnaik S, Becht E, Mezheyeuski A, et al. Cancer stemness, intra-tumoral heterogeneity, and immune response across cancers. Proc Natl Acad Sci U S A. 2019; 116: 9020–9029. https://doi.org/10.1073/pnas.1818210116 PMID: 30996127

10. Malta TM, Sokolov A, Gentles AJ, Burzykowski T, Poisson L, Weinstein JN, et al. Machine Learning Identifies Stemness Features Associated with Oncogenic Dedifferentiation. Cell. 2018; 173: 338–354. e15. https://doi.org/10.1016/j.cell.2018.03.034 PMID: 29625051

11. Li Y, Wang Z, Ajani JA, Song S. Drug resistance and Cancer stem cells. Cell Commun Signal. 2021; 19: 19. https://doi.org/10.1186/s12964-020-00627-5 PMID: 33588867

12. Xiao B, Liu L, Chen Z, Li A, Xia Y, Wang P, et al. A Novel Overall Survival Prediction Signature Based on Cancer Stem Cell-Related Genes in Osteosarcoma. Front Cell Dev Biol. 2021; 9: 753414. https://doi.org/10.3389/fcell.2021.753414 PMID: 34733853

13. Ben-Porath I, Thomson MW, Carey VJ, Ge R, Bell GW, Regev A, et al. An embryonic stem cell-like gene expression signature in poorly differentiated aggressive human tumors. Nat Genet. 2008; 40: 499–507. https://doi.org/10.1038/ng.127 PMID: 18443585

14. Yang L, Shi P, Zhao G, Xu J, Peng W, Zhang J, et al. Targeting cancer stem cell pathways for cancer therapy. Signal Transduct Target Ther. 2020; 5: 8. https://doi.org/10.1038/s41392-020-0110-5 PMID: 32296030

15. Dragu DL, Necula LG, Bleotu C, Diaconu CC, Chivu-Economescu M. Therapies targeting cancer stem cells: Current trends and future challenges. World J Stem Cells. 2015; 7: 1185–201. https://doi.org/10.4252/wjsc.v7.i9.1185 PMID: 26516409

16. Sun HR, Wang S, Yan SC, Zhang Y, Nelson PJ, Jia HL, et al. Therapeutic strategies targeting cancer stem cells and their microenvironment. Front Oncol. 2019; 9: 1104. https://doi.org/10.3389/fonc.2019.01104 PMID: 31709180

17. Wang J, Ren H, Wu W, Zeng Q, Chen J, Han J, et al. Immune Infiltration, Cancer Stemness, and Targeted Therapy in Gastrointestinal Stromal Tumor. Front Immunol. 2021; 12: 691713. https://doi.org/10.3389/fimmu.2021.691713 PMID: 34925310

18. Chen P, Hsu WH, Han J, Xia Y, DePinho RA. Cancer Stemness Meets Immunity: From Mechanism to Therapy. Cell Rep. 2021; 34: 108597. https://doi.org/10.1016/j.celrep.2020.108597 PMID: 33406434

19. Zhang H, Steed A, Co M, Chen X. Cancer stem cells, epithelial-mesenchymal transition, ATP and their roles in drug resistance in cancer. Cancer Drug Resist. 2021; 4: 684–709. https://doi.org/10.20517/cdr.2021.32 PMID: 34322664

20. Zhang SC, Hu ZQ, Long JH, Zhu GM, Wang Y, Jia Y, et al. Clinical implications of tumor-infiltrating immune cells in breast cancer. J Cancer. 2019; 10: 6175–6184. https://doi.org/10.7150/jca.35901 PMID: 31762828

21. Hu X, Wu L, Liu B, Chen K. Immune Infiltration Subtypes Characterization and Identification of Prognosis-Related lncRNAs in Adenocarcinoma of the Esophagogastric Junction. Front Immunol. 2021; 12: 651056. https://doi.org/10.3389/fimmu.2021.651056 PMID: 34122409

22. Zuo S, Wei M, Wang S, Dong J, Wei J. Pan-Cancer Analysis of Immune Cell Infiltration Identifies a Prognostic Immune-Cell Characteristic Score (ICCS) in Lung Adenocarcinoma. Front Immunol. 2020; 11: 1218. https://doi.org/10.3389/fimmu.2020.01218 PMID: 32714316

23. Andreou T, Rippaus N, Wronski K, Williams J, Taggart D, Cherqui S, et al. Hematopoietic Stem Cell Gene Therapy for Brain Metastases Using Myeloid Cell-Specific Gene Promoters. J Natl Cancer Inst. 2020; 112: 617–627. https://doi.org/10.1093/jnci/djz181 PMID: 31501884

24. Raniszewska A, Kwiecień I, Rutkowska E, Rzepecki P, Domagała-Kulawik J. Lung cancer stem cells—origin, diagnostic techniques and perspective for therapies. Cancers (Basel). 2021; 13: 2996. https://doi.org/10.3390/cancers13122996 PMID: 34203877

25. Parker KH, Beury DW, Ostrand-Rosenberg S. Myeloid-Derived Suppressor Cells: Critical Cells Driving Immune Suppression in the Tumor Microenvironment. Adv Cancer Res. 2015; 128: 95–139. https://doi.org/10.1016/bs.acr.2015.04.002 PMID: 26216631

26. Kumar V, Patel S, Tcyganov E, Gabrilovich DI. The Nature of Myeloid-Derived Suppressor Cells in the Tumor Microenvironment. Trends Immunol. 2016; 37: 208–220. https://doi.org/10.1016/j.it.2016.01.004 PMID: 26858199

27. Ellyard JI, Simson L, Parish CR. Th2-mediated anti-tumour immunity: Friend or foe? Tissue Antigens. 2007; 70: 1–11. https://doi.org/10.1111/j.1399-0039.2007.00869.x PMID: 17559575

28. Zhao X, Liu J, Ge S, Chen C, Li S, Wu X, et al. Saikosaponin A inhibits breast cancer by regulating Th1/Th2 balance. Front Pharmacol. 2019; 10: 624. https://doi.org/10.3389/fphar.2019.00624 PMID: 31214035

29. Knutson KL, Disis ML. Tumor antigen-specific T helper cells in cancer immunity and immunotherapy. Cancer Immunol Immunother. 2005; 54: 721–728. https://doi.org/10.1007/s00262-004-0653-2 PMID: 16010587

30. Zeng H, Ji J, Song X, Huang Y, Li H, Huang J, et al. Stemness Related Genes Revealed by Network Analysis Associated With Tumor Immune Microenvironment and the Clinical Outcome in Lung Adenocarcinoma. Front Genet. 2020; 11: 549213. https://doi.org/10.3389/fgene.2020.549213 PMID: 33193623

31. Hashemi ZS, Moghadam MF, Farokhimanesh S, Rajabibazl M, Sadroddiny E. Inhibition of breast cancer metastasis by co-transfection of miR-31/193b-mimics. Iran J Basic Med Sci. 2018; 21: 427–433. https://doi.org/10.22038/IJBMS.2018.26614.6522 PMID: 29796229

32. Bishop E. MicroRNAs: Genomics, biogenesis, mechanism, and function. Cell. 2004; 116: 281–97. https://doi.org/10.1016/s0092-8674(04)00045-5 PMID: 14744438

33. Fu Z, Wang L, Li S, Chen F, Au-Yeung KKW, Shi C. MicroRNA as an Important Target for Anticancer Drug Development. Front Pharmacol. 2021; 12: 736323. https://doi.org/10.3389/fphar.2021.736323 PMID: 34512363

34. Gao P, Xing AY, Zhou GY, Zhang TG, Zhang JP, Gao C, et al. The molecular mechanism of microRNA-145 to suppress invasion-metastasis cascade in gastric cancer. Oncogene. 2013; 32: 491–501. https://doi.org/10.1038/onc.2012.61 PMID: 22370644

35. Dzobo K, Senthebane DA, Ganz C, Thomford NE, Wonkam A, Dandara C. Advances in Therapeutic Targeting of Cancer Stem Cells within the Tumor Microenvironment: An Updated Review. Cells. 2020; 9: 1896. https://doi.org/10.3390/cells9081896 PMID: 32823711

36. Sokolov A, Paull EO, Stuart JM. One-class detection of cell states in tumor subtypes. Pacific Symp Biocomput. 2016; 21: 405–416. https://doi.org/10.1142/9789814749411_0037 PMID: 26776204

37. Qian D, Qian C, Ye B, Xu M, Wu D, Li J, et al. Development and Validation of a Novel Stemness-Index-Related Long Noncoding RNA Signature for Breast Cancer Based on Weighted Gene Co-Expression Network Analysis. Front Genet. 2022; 13: 760514. https://doi.org/10.3389/fgene.2022.760514 PMID: 35273635

38. Tang R, Liu X, Wang W, Hua J, Xu J, Liang C, et al. Identification of the Roles of a Stemness Index Based on mRNA Expression in the Prognosis and Metabolic Reprograming of Pancreatic Ductal Adenocarcinoma. Front Oncol. 2021; 11: 643465. https://doi.org/10.3389/fonc.2021.643465 PMID: 33912458

39. Chen X, Zhang D, Jiang F, Shen Y, Li X, Hu X, et al. Prognostic Prediction Using a Stemness Index-Related Signature in a Cohort of Gastric Cancer. Front Mol Biosci. 2020; 7: 570702. https://doi.org/10.3389/fmolb.2020.570702 PMID: 33134315

40. Tan J, Zhu H, Tang G, Liu H, Wanggou S, Cao Y, et al. Molecular Subtypes Based on the Stemness Index Predict Prognosis in Glioma Patients. Front Genet. 2021; 12: 616507. https://doi.org/10.3389/fgene.2021.616507 PMID: 33732284

41. Yuan H, Yu Q, Pang J, Chen Y, Sheng M, Tang W. The Value of the Stemness Index in Ovarian Cancer Prognosis. Genes (Basel). 2022; 13: 993. https://doi.org/10.3390/genes13060993 PMID: 35741755

42. Xia X, Li Y. Comprehensive analysis of transcriptome data stemness indices identifies key genes for controlling cancer stem cell characteristics in gastric cancer. Transl Cancer Res. 2020; 9: 6050–6061. https://doi.org/10.21037/tcr-20-704 PMID: 35117216

43. Guo L, Li H, Li W, Tang J. Construction and investigation of a combined hypoxia and stemness index lncRNA-associated ceRNA regulatory network in lung adenocarcinoma. BMC Med Genomics. 2020; 13: 166. https://doi.org/10.1186/s12920-020-00816-8 PMID: 33148251

44. Chen Z, Tang W, Zhou Y, He Z. The role of LINC01419 in regulating the cell stemness in lung adenocarcinoma through recruiting EZH2 and regulating FBP1 expression. Biol Direct. 2022; 17: 23. https://doi.org/10.1186/s13062-022-00336-8 PMID: 36050791

45. Weinstein JN, Collisson EA, Mills GB, Shaw KRM, Ozenberger BA, Ellrott K, et al. The cancer genome atlas pan-cancer analysis project. Nat Genet. 2013; 45: 1113–1120. https://doi.org/10.1038/ng.2764 PMID: 24071849

46. Barrett T, Wilhite SE, Ledoux P, Evangelista C, Kim IF, Tomashevsky M, et al. NCBI GEO: Archive for functional genomics data sets—Update. Nucleic Acids Res. 2013; 41: D991–D995. https://doi.org/10.1093/nar/gks1193 PMID: 23193258

47. Cerami E, Gao J, Dogrusoz U, Gross BE, Sumer SO, Aksoy BA, et al. The cBio Cancer Genomics Portal: An open platform for exploring multidimensional cancer genomics data. Cancer Discov. 2012; 2: 401–404. https://doi.org/10.1158/2159-8290.CD-12-0095 PMID: 22588877

48. Love MI, Huber W, Anders S. Moderated estimation of fold change and dispersion for RNA-seq data with DESeq2. Genome Biol. 2014; 15: R106. https://doi.org/10.1186/s13059-014-0550-8 PMID: 25516281

49. Ritchie ME, Phipson B, Wu D, Hu Y, Law CW, Shi W, et al. Limma powers differential expression analyses for RNA-sequencing and microarray studies. Nucleic Acids Res. 2015; 43: e47. https://doi.org/10.1093/nar/gkv007 PMID: 25605792

50. Blagoev KB, Wilkerson J, Fojo T. Hazard ratios in cancer clinical trials-a primer. Nat Rev Clin Oncol. 2012; 9: 178–183. https://doi.org/10.1038/nrclinonc.2011.217 PMID: 22290283

51. Li T, Fu J, Zeng Z, Cohen D, Li J, Chen Q, et al. TIMER2.0 for analysis of tumor-infiltrating immune cells. Nucleic Acids Res. 2020; 48: W509–W514. https://doi.org/10.1093/nar/gkaa407 PMID: 32442275

52. Li B, Severson E, Pignon JC, Zhao H, Li T, Novak J, et al. Comprehensive analyses of tumor immunity: Implications for cancer immunotherapy. Genome Biol. 2016; 17: 174. https://doi.org/10.1186/s13059-016-1028-7 PMID: 27549193

53. Jiang P, Gu S, Pan D, Fu J, Sahu A, Hu X, et al. Signatures of T cell dysfunction and exclusion predict cancer immunotherapy response. Nat Med. 2018; 24: 1550–1558. https://doi.org/10.1038/s41591-018-0136-1 PMID: 30127393

54. Becht E, Giraldo NA, Lacroix L, Buttard B, Elarouci N, Petitprez F, et al. Erratum to Estimating the population abundance of tissue-infiltrating immune and stromal cell populations using gene expression [Genome Biol., 17 (2016), (218)]. Genome Biol. 2016; 17: 218. https://doi.org/10.1186/s13059-016-1113-y PMID: 27908289

55. Finotello F, Mayer C, Plattner C, Laschober G, Rieder Di, Hackl H, et al. Molecular and pharmacological modulators of the tumor immune contexture revealed by deconvolution of RNA-seq data. Genome Med. 2019; 11: 34. https://doi.org/10.1186/s13073-019-0638-6 PMID: 31126321

56. Aran D, Hu Z, Butte AJ. xCell: Digitally portraying the tissue cellular heterogeneity landscape. Genome Biol. 2017; 18: 220. https://doi.org/10.1186/s13059-017-1349-1 PMID: 29141660

57. Newman AM, Liu CL, Green MR, Gentles AJ, Feng W, Xu Y, et al. Robust enumeration of cell subsets from tissue expression profiles. Nat Methods. 2015; 12: 453–457. https://doi.org/10.1038/nmeth.3337 PMID: 25822800

58. Racle J, de Jonge K, Baumgaertner P, Speiser DE, Gfeller D. Simultaneous enumeration of cancer and immune cell types from bulk tumor gene expression data. Elife. 2017; 6: e26476. https://doi.org/10.7554/eLife.26476 PMID: 29130882

59. Sturm G, Finotello F, Petitprez F, Zhang JD, Baumbach J, Fridman WH, et al. Comprehensive evaluation of transcriptome-based cell-type quantification methods for immuno-oncology. Bioinformatics. 2019; 35: i436–i445. https://doi.org/10.1093/bioinformatics/btz363 PMID: 31510660

60. Sticht C, De La Torre C, Parveen A, Gretz N. Mirwalk: An online resource for prediction of microrna binding sites. PLoS One. 2018; 13: e0206239. https://doi.org/10.1371/journal.pone.0206239 PMID: 30335862

61. Huang HY, Lin YCD, Li J, Huang KY, Shrestha S, Hong HC, et al. MiRTarBase 2020: Updates to the experimentally validated microRNA-target interaction database. Nucleic Acids Res. 2020; 48: D148–D154. https://doi.org/10.1093/nar/gkz896 PMID: 31647101

62. Fu J, Li K, Zhang W, Wan C, Zhang J, Jiang P, et al. Large-scale public data reuse to model immunotherapy response and resistance. Genome Med. 2020; 12: 21. https://doi.org/10.1186/s13073-020-0721-z PMID: 32102694

63. Lin J, Zheng X, Tian X, Guan J, Shi H. miR-1247-3p targets STAT5A to inhibit lung adenocarcinoma cell migration and chemotherapy resistance. J Cancer. 2022; 13: 2040–2049. https://doi.org/10.7150/jca.65167 PMID: 35517418

64. Tatsumi Y, Ohta S, Kimura H, Tsurimoto T, Obuse C. The ORC1 cycle in human cells: I. Cell cycle-regulated oscillation of human ORC1. J Biol Chem. 2003; 278: 41528–41534. https://doi.org/10.1074/jbc.M307534200 PMID: 12909627

65. Okano-Uchida T, Kent LN, Ouseph MM, McCarty B, Frank JJ, Kladney R, et al. Endoreduplication of the mouse genome in the absence of ORC1. Genes Dev. 2018; 32: 978–990. https://doi.org/10.1101/gad.311910.118 PMID: 29967292

66. Suo HD, Tao Z, Zhang L, Jin ZN, Li XY, Ma W, et al. Coexpression Network Analysis of Genes Related to the Characteristics of Tumor Stemness in Triple-Negative Breast Cancer. Biomed Res Int. 2020; 2020: 7575862. https://doi.org/10.1155/2020/7575862 PMID: 32766313

67. Wu B, Xi S. Bioinformatics analysis of the transcriptional expression of minichromosome maintenance proteins as potential indicators of survival in patients with cervical cancer. BMC Cancer. 2021; 21: 928. https://doi.org/10.1186/s12885-021-08674-y PMID: 34404366

68. Han L, Li F. Origin recognition complex subunit 1 (ORC1) augments malignant behaviors of lung adenocarcinoma cells via targeting Wnt signaling. Bioengineered. 2022; 13: 13520–13533. https://doi.org/10.1080/21655979.2022.2078562 PMID: 36700467

69. Jian Y, Qiao Q, Tang J, Xiaobing QIN. Origin recognition complex 1 regulates phospholipase Cδ1 to inhibit cell proliferation, migration and epithelial-mesenchymal transition in lung adenocarcinoma. Oncol Lett. 2022; 24: 252. https://doi.org/10.3892/ol.2022.13372 PMID: 35761947

70. Galluzzi L, Spranger S, Fuchs E, López-Soto A. WNT Signaling in Cancer Immunosurveillance. Trends Cell Biol. 2019; 29: 44–65. https://doi.org/10.1016/j.tcb.2018.08.005 PMID: 30220580

71. Li K, Shi H, Zhang B, Ou X, Ma Q, Chen Y, et al. Myeloid-derived suppressor cells as immunosuppressive regulators and therapeutic targets in cancer. Signal Transduct Target Ther. 2021; 6: 362. https://doi.org/10.1038/s41392-021-00670-9 PMID: 34620838

72. Wang Y, Ding Y, Guo N, Wang S. MDSCs: Key criminals of tumor pre-metastatic niche formation. Front Immunol. 2019; 10: 172. https://doi.org/10.3389/fimmu.2019.00172 PMID: 30792719

73. Feng S, Cheng X, Zhang L, Lu X, Chaudhary S, Teng R, et al. Myeloid-derived suppressor cells inhibit T cell activation through nitrating LCK in mouse cancers. Proc Natl Acad Sci U S A. 2018; 115: 10094–10099. https://doi.org/10.1073/pnas.1800695115 PMID: 30232256

74. Condamine T, Ramachandran I, Youn JI, Gabrilovich DI. Regulation of tumor metastasis by myeloid-derived suppressor cells. Annu Rev Med. 2015; 66: 97–110. https://doi.org/10.1146/annurev-med-051013-052304 PMID: 25341012

75. Vetsika EK, Koukos A, Kotsakis A. Myeloid-derived suppressor cells: Major figures that shape the immunosuppressive and angiogenic network in cancer. Cells. 2019; 8: 1647. https://doi.org/10.3390/cells8121647 PMID: 31847487

76. Shi H, Li K, Ni Y, Liang X, Zhao X. Myeloid-Derived Suppressor Cells: Implications in the Resistance of Malignant Tumors to T Cell-Based Immunotherapy. Front Cell Dev Biol. 2021; 9: 707198. https://doi.org/10.3389/fcell.2021.707198 PMID: 34336860

77. Ren X, Chen X, Ji Y, Li L, Li Y, Qin C, et al. Upregulation of KIF20A promotes tumor proliferation and invasion in renal clear cell carcinoma and is associated with adverse clinical outcome. Aging (Albany NY). 2020; 12: 25878–25894. https://doi.org/10.18632/aging.202153 PMID: 33232285

78. Tang N, Dou X, You X, Shi Q, Ke M, Liu G. Pan-cancer analysis of the oncogenic role of discs large homolog associated protein 5 (DLGAP5) in human tumors. Cancer Cell Int. 2021; 21: 457. https://doi.org/10.1186/s12935-021-02155-9 PMID: 34454476

79. Ding N, Li R, Shi W, He C. CENPI is overexpressed in colorectal cancer and regulates cell migration and invasion. Gene. 2018; 674: 80–86. https://doi.org/10.1016/j.gene.2018.06.067 PMID: 29936263

80. Branchi V, García SA, Radhakrishnan P, Győrffy B, Hissa B, Schneider M, et al. Prognostic value of DLGAP5 in colorectal cancer. Int J Colorectal Dis. 2019; 34: 1455–1465. https://doi.org/10.1007/s00384-019-03339-6 PMID: 31286215

81. Li K, Fu X, Wu P, Zhaxi B, Luo H, Li Q. DLG7/DLGAP5 as a potential therapeutic target in gastric cancer. Chin Med J (Engl). 2022; 135: 1616–1618. https://doi.org/10.1097/CM9.0000000000001859 PMID: 35075051

82. Yi JM, Eun Jin, Hyun Mi, Bae JH, Kang K, Ahuja N, et al. Epigenetically altered miR-1247 functions as a tumor suppressor in pancreatic cancer. Oncotarget. 2017; 8: 26600–26612. https://doi.org/10.18632/oncotarget.15722 PMID: 28460450

83. Zhang P, Fan C, Du J, Mo X, Zhao Q. Association of miR-1247-5p expression with clinicopathological parameters and prognosis in breast cancer. Int J Exp Pathol. 2018; 99: 199–205. https://doi.org/10.1111/iep.12287 PMID: 30175411

84. Fang T, Lv H, Lv G, Li T, Wang C, Han Q, et al. Tumor-derived exosomal miR-1247-3p induces cancer-associated fibroblast activation to foster lung metastasis of liver cancer. Nat Commun. 2018; 9: 191. https://doi.org/10.1038/s41467-017-02583-0 PMID: 29335551

85. Wei QF, Yao JS, Yang Y. MicroRNA-1247 inhibits the viability and metastasis of osteosarcoma cells via targeting NRP1 and mediating Wnt/β-catenin pathway. Eur Rev Med Pharmacol Sci. 2019; 23: 7266–7274. https://doi.org/10.26355/eurrev_201909_18831 PMID: 31539113

86. Wu T, Lin Y, Xie Z. MicroRNA-1247 inhibits cell proliferation by directly targeting ZNF346 in childhood neuroblastoma. Biol Res. 2018; 51: 13. https://doi.org/10.1186/s40659-018-0162-y PMID: 29793538

87. Svoronos AA, Engelman DM, Slack FJ. OncomiR or tumor suppressor? The duplicity of MicroRNAs in cancer. Cancer Res. 2016; 76: 3666–3670. https://doi.org/10.1158/0008-5472.CAN-16-0359 PMID: 27325641